

### 3-D depth migration operators for marine controlled-source electromagnetic data

Tage Røsten\*, Ketil Hokstad and Børge Arntsen, Statoil Research Centre, N-7005 Trondheim, Norway

#### Summary

Electromagnetic diffusive fields and seismic wave fields can both be propagated in smooth background media using Helmholtz-type equations. Consequently, many seismic migration methods operating in the frequency-space domain can be adapted for controlled-source electromagnetic (CSEM) data. We present and demonstrate 3-D frequency-wavenumber and explicit finite-difference depth migration operators optimized for the electric field. Rapid numerical implementation was possible by modification of an existing seismic 3-D depth migration code running on massive Linux clusters. Results from numerical extrapolation of the electric field from a Hertz dipole compare well with the analytical solution. The CSEM depth migration code runs three orders of magnitude faster than the seismic code.

#### Introduction

During the last few years, marine controlled-source electromagnetic (CSEM) data, often called seabed logging (SBL), has been widely used by the oil and gas industry for remote detection of hydrocarbon (HC) reservoirs. EM energy is rapidly attenuated in the sea water and in sediments where the pore space is filled with conductive brine. In high-resistive (low-conductive) layers such as HC-filled sandstones, the EM field is assumed to be refracted and guided along the high-resistive layers with less attenuation. Energy is constantly refracted back to the sea floor and detected by EM receivers. A major objective of marine CSEM processing is to image conductivity anomalies in depth, by means of migration or inversion. Usually, the fundamental frequency and a few harmonics can be utilized in the imaging. In the preprocessing of the data, the up-going scattered field due to the resistivity anomalies should be separated from the total field, which also include the direct wave and the air wave.

If the background medium is sufficiently smooth, the propagation properties of both seismic and EM fields can be represented in the frequency-space ( $FX$ ) domain by Helmholtz-type differential equations. Consequently, similar migration schemes can be applied to both types of data. Most  $FX$ -domain migration schemes developed for seismic imaging can easily be adapted for depth migration of CSEM data. In isotropic background media, the dispersion relations of seismic and EM fields are formally equal. There are, however, important details that are different, and must be accounted for. The seismic wavenum-

ber is real and depends linearly on frequency, whereas the EM wavenumber is complex and proportional to the square-root of the temporal frequency. Consequently, the propagation of the EM field is governed by a diffusive wave equation. Another issue of major importance is the difference in phase properties of 2-D and 3-D field extrapolators. Seismic data are recorded in the far field, where the 2-D phase is an excellent approximation to the 3-D phase of the field data. Hence seismic 2-D lines can be migrated using 2-D schemes. For CSEM data, near-field effects are important, and the phase of 2-D and 3-D field extrapolators differ significantly. CSEM data are often acquired with 2-D line geometries. However, in the imaging it is important to account for the 3-D nature of the EM fields, either by means of full 3-D migration or inversion schemes, or by applying appropriate corrections (Stoyer and Greenfield, 1976; Hokstad and Røsten, 2006). Correct handling of the phase of the (diffusive) wavefields is crucial in any depth migration scheme. Otherwise, target anomalies may image at the wrong depth.

Zhdanov et al. (1996) introduced depth migration for marine CSEM data, based on Gazdag's frequency-wavenumber ( $FK$ ) migration and Claerbout's 45-degree finite-difference ( $FD$ ) equation (Claerbout, 1985). The 45-degree  $FD$  equation can easily be implemented in 2-D, where an implicit Crank-Nicholson scheme leads to linear tridiagonal systems of equations to be solved for the wavefield. The corresponding 3-D scheme becomes more cumbersome, since banded matrices must be inverted to solve for the downward-continued fields. Here, we present and compare schemes for 3-D  $FK$  migration and 3-D explicit  $FD$  depth migration of marine CSEM data. Following the approach to seismic depth migration of Holberg (1988), we design optimized convolution-based filters for downward continuation of the electric field. The filter design can easily be extended to include anisotropy, using the equations presented by Hokstad and Røsten (2006). The magnetic field can be handled with the same approach.

The novel 3-D EM migration code was developed by modification of an existing 3-D seismic depth migration code running in parallel under the Message Passing Interface (MPI) on massive Linux clusters. This allowed for very rapid implementation of the EM migration scheme, since only minor modifications of the code were required. Because coarser spatial grids can be used, and fewer temporal frequencies are available, the CSEM version of the code runs three orders of magnitudes faster than the seismic code.

#### One-way equations for the electric field

In the ultra-low frequency approximation, the Maxwell

### 3-D depth migration operators for marine CSEM data

equations in the frequency domain can be written as

$$\nabla \times \mathbf{E} = i\omega\mu_0\mathbf{H}, \quad (1)$$

$$\nabla \times \mathbf{H} = \mathbf{J}, \quad (2)$$

where  $\mathbf{E}$  is the electric field,  $\mathbf{H}$  is the magnetic field,  $\mu_0$  is the vacuum permeability, and  $\omega$  is the angular frequency. We assume a linear medium, zero source current density, and that the conduction current density  $\mathbf{J}$  is given by Ohm's law

$$\mathbf{J} = \sigma\mathbf{E}, \quad (3)$$

where  $\sigma$  is the conductivity. Combining the equations above to eliminate the  $\mathbf{H}$ -field, and assuming a charge-free medium such that  $\partial_i E_i = 0$ , we obtain the Helmholtz equation

$$\nabla^2 E_i + \kappa_0^2 E_i = 0, \quad (4)$$

for each component  $E_i$  of the electric field. The same equation is the basis for seismic migration. In the seismic case,  $\kappa_0$  is real, but in the CSEM case, the wavenumber

$$\kappa_0 = \sqrt{i\omega\mu_0\sigma}, \quad (5)$$

is complex, which leads to (strong) attenuation. The adjoint Helmholtz equation is obtained by changing the sign of the last term in equation (4).

Assuming a 1-D background medium, and Fourier transforming over the horizontal spatial coordinates, equation (4) readily leads to one-way way equations in the  $FK$  domain for down-going fields  $E_i^D$  and up-going fields  $E_i^U$ . From the adjoint Helmholtz equation, we correspondingly obtain a one-way equation for the so-called migrated field  $E_i^M$ , introduced by Zhdanov et al. (1996). The migrated field is equal to the up-going field at the recording surface  $z = z_r$ , but differs elsewhere. The  $FK$ -domain one-way equation can be written as

$$\partial_z E_i^\nu = \gamma k_z E_i^\nu, \quad (6)$$

where

$$k_z = \sqrt{\kappa_0^2 + \gamma^2(k_x^2 + k_y^2)}, \quad (7)$$

is the vertical wavenumber, and

$$\gamma = \begin{cases} i & \text{for } \nu = D, \\ -i & \text{for } \nu = U, \\ -1 & \text{for } \nu = M. \end{cases} \quad (8)$$

The sign convention in the Fourier transform is such that  $\partial_t \leftrightarrow -i\omega$  and  $\partial_i \leftrightarrow ik_i$ . The solution to equation (6) is given by

$$E_i^\nu(k_x, k_y, z + \Delta z) = e^{\gamma\Delta z k_z} E_i^\nu(k_x, k_y, z), \quad (9)$$

which is the basis for the wavefield extrapolation step of (Gazdag)  $FK$  migration. The depth-stepping equation for  $E_i^D$  decays exponentially, and is numerically stable. The equation for  $E_i^U$  is exponentially growing and is numerically unstable. It can, however, be applied in

a “phase-only” migration scheme, if only the real part of the vertical wavenumber  $k_z$  is used in the downward continuation. The depth-stepping equation for  $E_i^M$  is numerically stable with exponential decay (like  $E_i^D$ ) and backward phase rotation (like  $E_i^U$ ). The  $FK$  migration operators are accurate up to 90 degrees from the vertical, but limited to 1-D background media.

### 3-D filter operator design

To relax the 1-D background assumption, we replace the phase-shift operator in equation (9) by discrete 2-D convolution filters  $W^\nu(m\Delta x, n\Delta y, \hat{\kappa}_0)$  in the  $FX$  domain, as proposed by Holberg (1988). Then the extrapolation of the E-field can be written as

$$E_i^\nu(x, y, z + \Delta z) =$$

$$\sum_{m,n=-L}^L W^\nu(m\Delta x, n\Delta y, \hat{\kappa}_0) E_i^\nu(x - m\Delta x, y - n\Delta y, z). \quad (10)$$

The convolution operators depend only on the normalized wavenumber  $\hat{\kappa}_0 = \kappa_0\Delta x$  and the ratio  $\Delta z/\Delta x$ . Hence, for a given  $\Delta z/\Delta x$ -ratio, the operator coefficients can be precomputed for all relevant values of  $\hat{\kappa}_0$  and stored in a look-up table. For simplicity we assume  $\Delta y = \Delta x$  and  $\Delta z/\Delta x = 0.5$ . Computation of the finite impulse-response filter with complex-valued coefficients  $W^\nu(m\Delta x, n\Delta y, \hat{\kappa}_0)$ , is posed as an inverse problem, minimizing the objective function in the  $L_4$  norm

$$J = \|W^\nu(i\Delta k_x, j\Delta k_y, \hat{\kappa}_0) - e^{\gamma\Delta z k_z}\|^4, \quad (11)$$

where  $W^\nu(i\Delta k_x, j\Delta k_y, \hat{\kappa}_0)$  is the discrete 2-D spatial Fourier transform of  $W^\nu(m\Delta x, n\Delta y, \hat{\kappa}_0)$  for a discrete set of horizontal wavenumbers  $i\Delta k_x$  and  $j\Delta k_y$ .

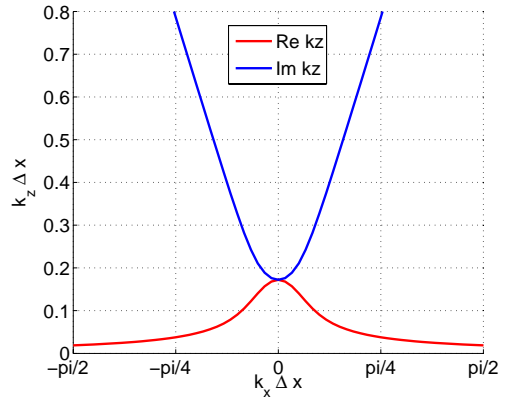


Fig. 1: Dispersion relation computed with  $\sigma = 1.0$  S/m and  $f = 0.75$  Hz and  $\gamma = i$ .

The seismic dispersion relation is discontinuous at the transition to the evanescent region where  $k_z = 0$ . Hence, the filter operators for seismic 3-D depth migration are

### 3-D depth migration operators for marine CSEM data

matched to propagating waves only by introducing a dip-limitation. The evanescent waves are damped to get a stable 3-D explicit depth migration scheme. The dispersion relations for diffusive EM fields are smooth and continuous for all wavenumbers, see Figure 1. Hence, we do not need to introduce a dip-limitation on the corresponding 3-D filter operators to get a stable depth migration scheme for CSEM data. The optimization is generally performed for all wavenumbers, and the real and imaginary part of the filter operator are optimized separately. In practice, we need to compute tabulated filter coefficients only for  $W_i^D$ . Then the operator for  $W_i^M$  can be obtained by complex conjugation.

Figures 2 shows the amplitude and phase responses for  $e^{i\Delta z k_z}$  (i.e. down-going operator) assuming  $\sigma = 1.0$  S/m and  $f = 0.75$  Hz. Figures 3 shows the corresponding amplitude and phase responses for the optimized 3-D spatial filters. In the filter design we used half-length  $L = 12$ , and the number of discrete positive horizontal wavenumbers was  $I = J = 64$ . Note the excellent match for both the magnitude and the phase.

#### Numerical examples

To demonstrate the 3-D *FK* and *FD* migration operators presented above, we propagate the  $x$ -component of an electric Hertz dipole oriented in the  $x$ -direction. The frequency of the dipole is 0.75 Hz, and the background medium is homogeneous with conductivity 1.0 S/m. For comparison and reference, Figure 4 shows the phase (in radians) of the analytical Hertz dipole in the vertical  $xz$ -plane containing the dipole source. The source is located at the origin.

We computed the dipole field analytically at 500 m depth below the source point, and propagated the field numerically from 500 m to 2000 m. The size of the numerical grid was  $N_x = N_y = N_z = 41$ , and the grid spacing was  $\Delta x = \Delta y = 100$  m and  $\Delta z = 50$  m.

Figure 5 shows the phase of the field after downward continuation with the *FK* and *FD* field extrapolators. Both amplitude and phase are accounted for in the propagation. As expected, the *FK* scheme is more accurate at large angles from the vertical. The *FD* scheme compares well with the analytical solution at small angles (up to approximately 45 degrees). At large angles, the *FD* results deviates from the correct solution. This is expected since this type of explicit migration operator is known to have a limited dip response (Holberg, 1988). Also, some edge effects are introduced due to the small size of the computational grid compared to the half-length of the extrapolation filter.

Figure 6 shows the results obtained with phase-only migration operators. In this example, only the real part of  $k_z$  was used in the *FK* scheme. The *FD* operator was designed to match the phase of the exponential function in equation (11), with unit magnitude for all horizontal wavenumbers. The phase-only migration operators do not

handle the phase of the electric field correctly.

#### Discussion and conclusions

We have presented 3-D *FK* and 3-D explicit *FD* depth migration operators optimized for the electric field. The migration operators were demonstrated by numerical downward extrapolation of the electric field of a Hertz dipole. When both amplitude and phase are accounted for in the extrapolation, the numerical results compare well with the analytical solution. 3-D explicit one-way *FD* operators are known to have a limited dip response. As expected, the numerical results obtained with the *FD* scheme deviates from the correct solution at large angles from the vertical. Currently, we use convolution filters optimized for CSEM data, but with the same filter length as for the seismic case. This can probably be improved.

Extrapolation with phase-only operators, accounting for only the real part of the vertical wavenumber, did not give acceptable results. The phase of the downward-continued E-field becomes incorrect when migration operators with unit magnitude response are used.

The 3-D *FK* and *FD* migration schemes were implemented by modification of an existing seismic 3-D depth migration code running in parallel on Linux clusters. The CSEM depth migration code is very efficient and runs three orders of magnitude faster than the seismic code. This is due to the coarser spatial grids and fewer frequencies used in migration of CSEM data.

#### Acknowledgments

We thank Statoil for permission to publish this work.

#### References

- Claerbout, J.F., 1985, Imaging the earth's interior: Blackwell Sci. Publ.
- Hokstad, K., and Røsten, T., 2005, Anisotropic depth migration of marine controlled-source electromagnetic data: 68th Internat. Mtg., Eur. Assn. Geosci. Eng., A012.
- Holberg, O., 1988, Towards optimum one-way wave propagation: Geophys. Prosp., **36**, 99–114.
- Stoyer, C.H., and Greenfield, R.J., 1976, Numerical solutions of the response of a two-dimensional earth to an oscillating magnetic dipole source: Geophysics, **41**, 519–530.
- Zhdanov, M.S., Traynin, P., and Booker, J., 1996, Underground imaging by frequency-domain electromagnetic migration: Geophysics, **61**, 666–682.

### 3-D depth migration operators for marine CSEM data

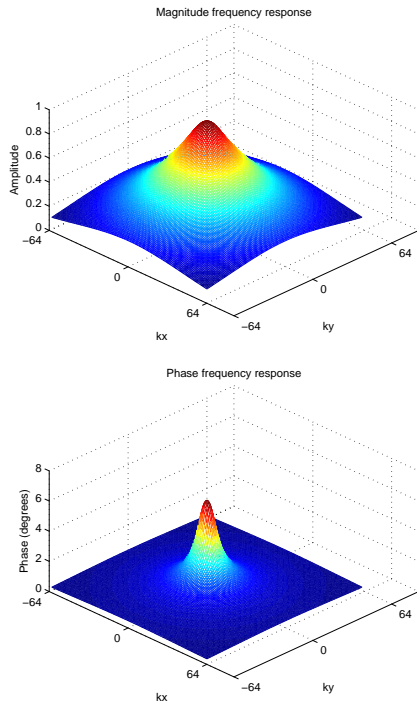


Fig. 2: Magnitude response (top) and phase response (bottom) of  $e^{\gamma \Delta z k_z}$  for  $\gamma = i$ .

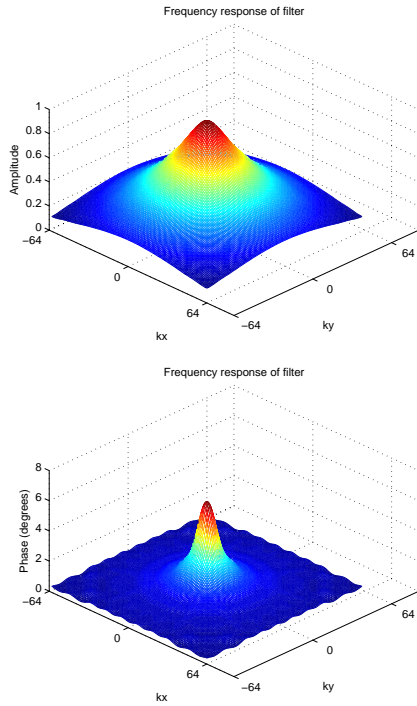


Fig. 3: Resulting magnitude response (top) and phase response (bottom) of  $W_i^D(k_x, k_y, k_0)$ .

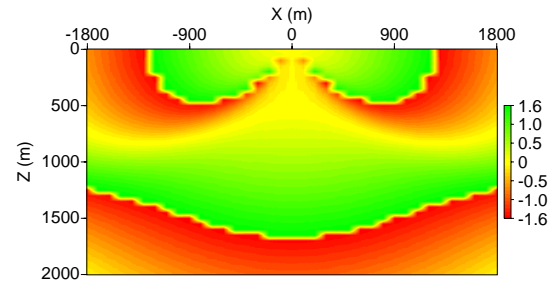


Fig. 4: Phase (in radians) of the inline horizontal ( $x$ ) component of an analytical free-space Hertz dipole. The frequency is 0.75 Hz and the conductivity is 1.0 S/m.

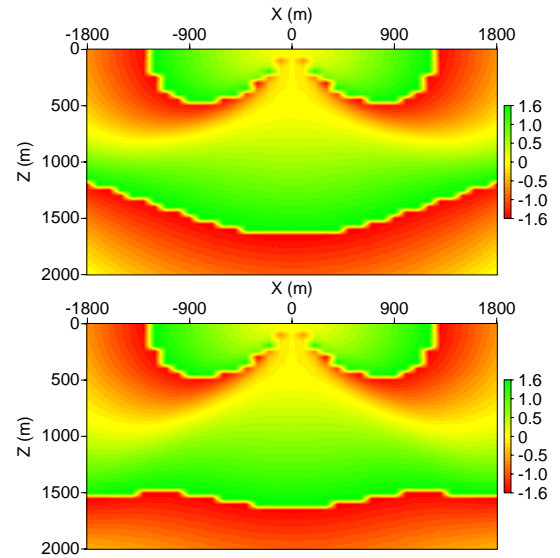


Fig. 5: Phase after downward continuation with the complete 3-D *FK* (top) and 3-D *FD* (bottom) migration operators.

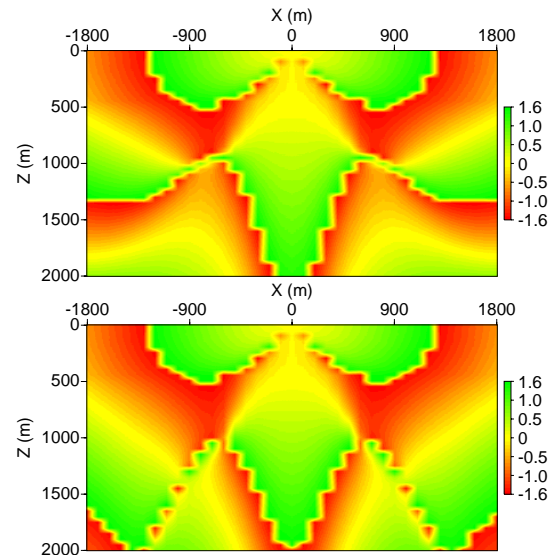


Fig. 6: Phase after downward continuation with the phase-only 3-D *FK* (top) and 3-D *FD* (bottom) migration operators.